


PCF-co-EF와 PLA 블렌드의 결정화 거동 및 열적 물성에 관한 연구

김한얼 · 남병욱[†] 

한국기술교육대학교 응용화학공학과

(2017년 11월 21일 접수, 2018년 1월 5일 수정, 2018년 2월 19일 채택)

Study on Crystallization Kinetics and Thermal Properties of PCF-co-EF/PLA Blends

Han Eol Kim and Byeong Uk Nam[†] 

Dept. of Applied Chemical Engineering, Korea University of Technology and Education, 1600 Chungjeol-ro, Cheonan 31253, Korea
(Received November 21, 2017; Revised January 5, 2018; Accepted February 19, 2018)

초록: 본 연구는 poly(cyclohexylenedimethylene furandicarboxylate-co-ethylene furandicarboxylate)(PCF-co-EF)와 poly(lactic acid)(PLA)를 블렌드하여 furan 기반의 바이오 복합재 개발을 목표로 하였다. PLA는 순수 PLA(4032D)와 첨가제가 마스터 배치된 PLA(3801X)를 사용하였다. FE-SEM을 통해 서브 마이크론의 구형 도메인 입자들이 복합재 내에 분산되어 있는 것을 통해 상용성을 확인하였고, 열적 물성 분석 및 비등온 결정화 거동 분석을 통해 PLA가 복합재의 결정화 속도를 가속시킨다는 것을 확인하였다. 또한 DMA를 이용한 동적 물성 측정을 통해 복합재의 상용성 및 연성의 향상을 확인하였다.

Abstract: The goal of this study is to develop furan based bio-composites by blending poly(cyclohexylenedimethylene furandicarboxylate-co-ethylene furandicarboxylate) (PCF-co-EF) with poly(lactic acid) (PLA). Two types of PLA are used in this study and one is neat PLA mostly consisting of L-lactide (4032D) and the other is master batched PLA with various additives (3801X). The FE-SEM results showed sub-micron dispersion of the spherical domains in the blends, which indicates compatibility between PCF-co-EF and PLA. The thermal properties and non-isothermal crystallization kinetics shows that the PLA accelerates the rate of crystallization. Dynamic mechanical analysis showed compatibility of the blends and the improvement of ductility of the composites.

Keywords: poly(cyclohexylenedimethylene furandicarboxylate-co-ethylene furandicarboxylate), poly(lactic acid), polymer blend, crystallization kinetics, thermal properties.

Introduction

Recently, renewable resources have attracted attention due to growing concerns for environment and depletion of fossil-fuel resources. To keep a pace with social issues, plastic industries show their interests to replace traditional fossil-fuel based plastics with renewable resource based plastics. Among them, poly(ethylene furandicarboxylate) (PEF) has been considered as a suitable bio-alternative to replace the poly(ethylene terephthalate) (PET).¹ In contrast to PET including terephthalic acid (TA) derived from fossil-fuel resources, PEF includes 2,5-

furandicarboxylic acid (FDCA) which was selected by U.S Department of Energy as one of the important bio-based building blocks to play an important role in the green chemical industry.² PEF has lower gas permeability for oxygen (O₂) and carbondioxide (CO₂) and easier processability related with its lower melting temperature (T_m) and higher glass transition temperature (T_g) than PET due to structural differences between FDCA and TA.³ Also, as it can be synthesized in a similar method to that of PET, it does not demand additional price when applying to PET manufacturing process. However, some drawbacks of PEF have been pointed out to its application. PEF shows brittle fracture behaviors that is caused by its rigid polymer chain and slower crystallization rate compared with that of PET. Moreover, its physical and thermal properties are still not enough to be commercialized, and its

[†]To whom correspondence should be addressed.
bunam@kut.ac.kr, ORCID[®] 0000-0001-5248-7349
©2018 The Polymer Society of Korea. All rights reserved.

price is also not yet to be comparable to other bio-based plastics.

Several researches have been proposed to solve drawbacks of PEF using long chain diol, such as propylene glycol,⁴ butylene glycol⁵⁻⁷ and hexylene glycol.⁸ With the incorporation of the long chain segment in the polymer chain, each furan based polyesters has a relatively low glass transition temperature, which could be considered as a brittle-to-ductile transition even if exact explanations are not mentioned. But, the longer the chain segment is, the more initial decomposition is expedited. Also, their low T_g according to chain length causes application limits in various area, and there is no effect on crystallization rate until C4 diol. Research on furan based polyesters is insufficient till now, moreover, researches on its copolymers or composites have been rarely tried.

Poly(lactic acid), (PLA), is an aliphatic polyester thermoplastic that is derived from biomass through bioconversion and polymerization. It has been viewed as one of the most promising materials because of its excellent biodegradability, thermal plasticity, and superior mechanical properties comparable to those of commercial biodegradable polymers.^{9,10} However, the applications of PLA as common plastics have been limited due to its drawbacks, such as the inherent brittleness and poor thermal stability. Thus, many attempts have been made to obtain PLA with improved properties, and various PLA composites has been commercialized.¹¹⁻¹³

The goal of this study is proposing a possibility of using new bio-composites based on furan based polyester as a promising alternative of fossil-based polyester. To solve some shortcomings of furan based-polyesters like slow crystallization rate, high cost and brittleness, PLA is melt blended with poly(cyclohexylenedimethylene furandicarboxylate-co-ethylene furandicarboxylate) (PCF-co-EF) which is a copolymer type of PEF. The reason for choosing PLA is its cost-effective performance compared with other commercial biodegradable polymers. Two types of PLA are used for blending; one is neat PLA mostly consisting of L-lactide and the other is master batched PLA with various additives. The neat PLA is selected for observing the compatibility and the property changes by PLA blending. Master batched PLA which has inorganic filler (talc) and additives is selected for observing the effects of inorganic filler as a crystallizer to accelerate the crystallization rate and the effects of additives as a plasticizer which is assumed to enhance the compatibility and ductility in PCF-co-EF/PLA blends system.

The phase morphology, crystallization characteristics, ther-

mal stability and relaxation transition behaviors of the blends were evaluated by field emission scanning electron microscopy (FE-SEM), differential scanning calorimetry (DSC), thermogravimetric analysis (TGA) and dynamic mechanical analysis (DMA).

Experimental

Materials. Poly(cyclohexylenedimethylene furandicarboxylate-co-ethylene furandicarboxylate) (PCF-co-EF) ($T_g=80^\circ\text{C}$, $T_m=235^\circ\text{C}$) was prepared by Lotte Chem Co., Korea. Two types of poly(lactic acid) were obtained from NatureWorks® LLC, USA; one is 4032D grade (neat PLA with 98.5% L-isomer lactide, $MI=3\text{ g/min}$, $T_g=62^\circ\text{C}$, $T_m=166^\circ\text{C}$), and the other is 3801X grade (modified PLA with talc, plasticizer and toughening agent, $MI=8\text{ g/min}$, $T_g=45^\circ\text{C}$, $T_m=164^\circ\text{C}$). All polymers were supplied in pellet form and used as received. To prevent the polymers from degradation during thermal processing, two antioxidants were added. The SONGNOX® 2450 is a phenolic antioxidant that is used as 1st antioxidant, and SONGNOX® 1680 is a phosphoric antioxidant that is used as 2nd antioxidant. Both antioxidants were obtained from Songwon Industrial Chem. Co., Korea.

Preparation of Blends. All materials were dried at 60°C for 24 hr prior to melt blending to minimize hydrolysis degradation, and the blends were prepared in a HAKKE Rheometer 600 p mixer with different PLA contents from 0 to 40 wt%. The processing conditions were kept constant with a processing temperature of 250°C and a rotor speed of 60 rpm during 10 min.

Analysis. In order to prepare specimens for analyses, all samples were compression-molded into 1 mm sheets at 250°C for 5 min under a pressure of 450 kgf/cm^2 . In order to obtain amorphous samples, all specimens were immediately quenched in cold water after the 5 min. All samples were dried overnight at 35°C under vacuum to remove residual water prior to measurement.

Field Emission Scanning Electronic Microscopy. Morphology of fracture surfaces were observed by field emission scanning electron microscopy (FE-SEM) using a JSM-7500F (JEOL Ltd., Japan). All specimens were fractured in liquid nitrogen and sputtered with a platinum coating before observation.

Differential Scanning Calorimetry. Thermal properties of the blends were investigated by differential scanning calorimetry (DSC, Perkin-Elmer Pyris Diamond) calibrated with

indium as a standard. All measurements were performed under N_2 atmosphere, and the sample weight was kept constant around 5.5 mg in all measurements. The measurement was carried out with two repeated cycles of a heating-cooling scan, and the first heating scan was ignored because it exhibited some noise due to the residual stresses from sample preparation. Samples were heated from 30 to 270 °C at 10 °C/min and held there for 5 min to eliminate residual crystals before cooling to 30 °C at 10 °C/min. Non-isothermal crystallization kinetics also investigated. Prior to investigating it, the equilibrium melting temperature (T_m^0) of neat PCF-co-EF was investigated using Hoffman-Weeks equation.¹⁴ Sample was heated from 30 to 270 °C at 10 °C/min and held there for 5 min before cooling to each crystallization temperature at maximum cooling rate. At each temperature, annealing lasted sufficiently, the samples were cooled down to 30 °C at a rate of 100 °C/min and then re-heated to 270 °C at a rate of 10 °C/min for the observation of the T_m . Non-isothermal crystallization kinetics were investigated based on Jeziorny method.¹⁵ Samples was heated from 30 to 270 °C at 10 °C/min and held there for 5 min. Subsequently, the samples were cooled to 30 °C at four different rates of 2.5, 5, 10, and 20 °C/min.

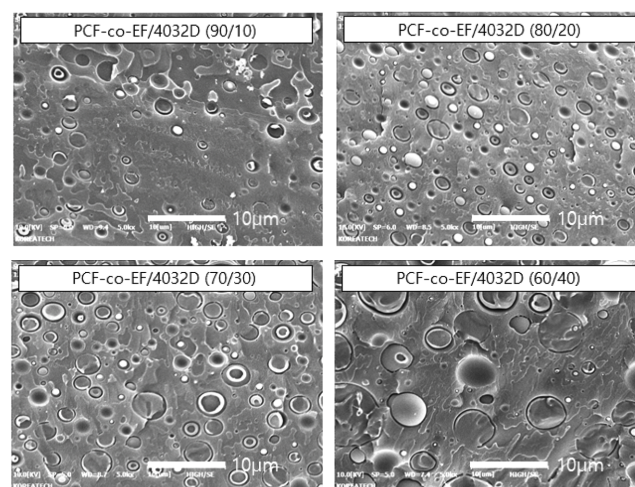
Thermogravimetric Analysis (TGA). To investigate the thermal stability of the blends, a thermogravimetric analysis (TGA4000, Perkin Elmer) was conducted from 30 to 800 °C at a heating rate of 20 °C/min under N_2 atmosphere.

Dynamic Mechanical Analysis (DMA). Thermal dynamic mechanical kinetics was analyzed on a DMA8000 (Perkin Elmer) to observe the relaxation temperature. The furnace was heated from -120 to 140 °C at 2 °C/min at a frequency of 1 Hz.

Results and Discussion

Phase Morphology of the Blends. The morphological development and stability of multiphase polymer blends are complex functions of the interfacial characteristics, blend composition, and shear conditions.¹⁶ In this study, all the blends show a matrix-droplet morphology, where the minor component exists as domain components as shown in Figure 1. In the 4032D blends, many spherical domain components are clearly observed in overall composition. Although it is well-known that polymer blends are completely homogeneous on the scale below 100 nm, sub-micron dispersion of the spherical domains also indicates compatibility of the blends.¹⁷ On the other hand, a relatively smooth fracture surface can be observed in the 3801X blends. It is supposed that the various

a) PCF-co-EF/PLA 4032D blends.



b) PCF-co-EF/PLA 3801X blends.

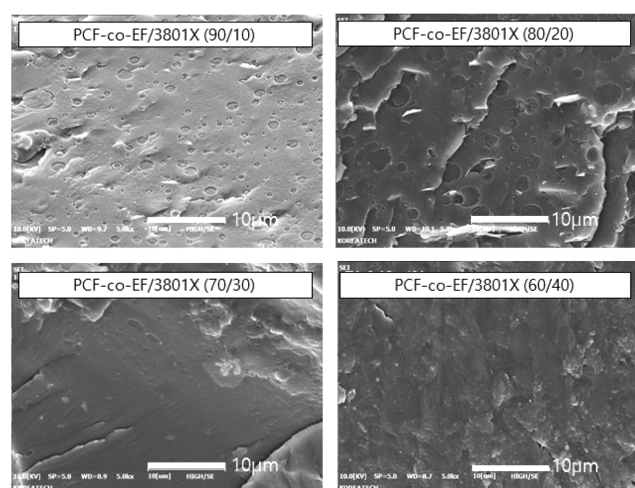


Figure 1. FE-SEM images of PCF-co-EF/PLA blends with different of PLA contents (scale bar=10 μm, ×5000): (a) PCF-co-EF/PLA(4032D) blends; (b) PCF-co-EF/PLA(3801X) blends.

additives in the PLA 3801X which are unknown exactly act as plasticizer and reduce the interfacial tension between the polymers, resulting in finer dispersion on the matrix.

Thermal Properties of the Blends. **Thermal Parameters of PCF-co-EF/PLA Blends:** Figure 2 shows the DSC thermograms for 4032D blends, and these results are summarized in Table 1. The behavior of T_g in the blends will be discussed in the dynamic mechanical analysis section since it is difficult to determine the T_g from DSC results. PCF-co-EF exhibited the T_g at 80 °C, T_{cc} at 141 °C, T_m at 235 °C, and T_{mc} at 154 °C. Inherent slow crystallization rate of furan based polyesters is improved to some extent due to existence of cyclohexanedi-methanol (CHDM) in main chain, but it is not yet to be suf-

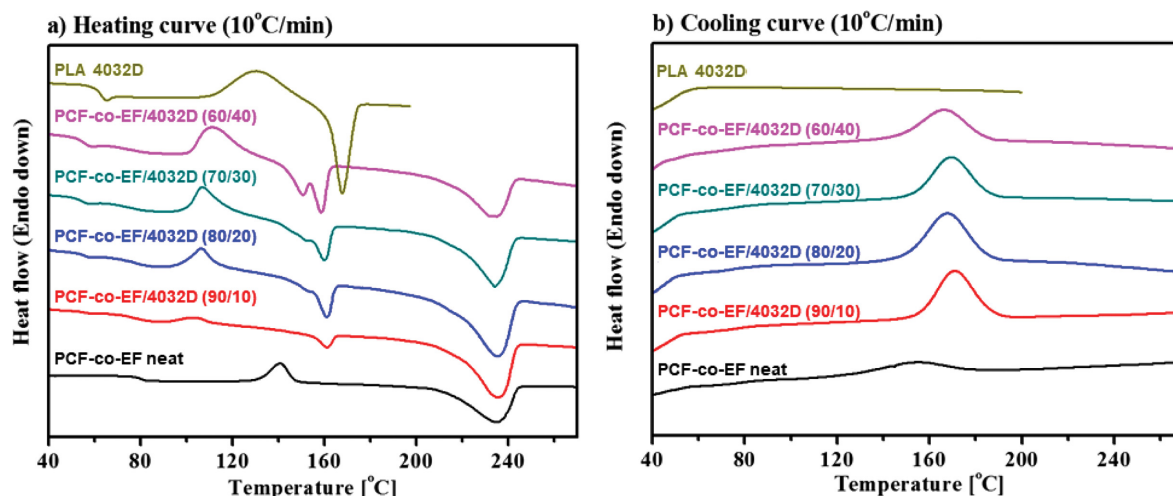


Figure 2. DSC thermograms of PCF-co-EF/PLA 4032D blends: (a) heating scan; (b) cooling scan.

Table 1. Thermal Transition Parameters of PCF-co-EF/PLA 4032D Blends

DSC (10 °C/min)	Heating				Cooling	
	T_g	T_{cc}	T_m	T_{mc}	T_m	T_{mc}
PLA 4032D	61	130	168	-		
PCF-co-EF/4032D (90/10)	53	78	110	-	150, 159	235
PCF-co-EF/4032D (80/20)	55	77	109	-	151, 160	234
PCF-co-EF/4032D (70/30)	56	78	106	-	152, 161	235
PCF-co-EF/4032D (60/40)	-	78	103	-	161	235
PCF-co-EF	80	141	235	154		

ficient for application in various areas. PLA 4032D exhibited the T_g at 61 °C, T_{cc} at 130 °C and T_m at 168 °C, and there is no observable peak on cooling scan. In the blends, the incorporation of the PLA resulted in no significant changes in T_m , but affected T_c . Crystallization of all blends was accelerated, but the amount of PLA had little effect on changes of T_c . All the blends have two endo-thermal peaks at 160 °C, which are related with melting of PLA crystals; the lower endo-thermal peak is related to melting of PLA crystals developed during the DSC slow cooling scan and the higher endo-thermal peak is related to melting of PLA crystals developed by gradual melting and recrystallization during the DSC heating scan.¹⁸ It is assumed that PLA 4032D formed perfect crystals under the influence of PCF-co-EF. Figure 3 shows the DSC thermograms for the 3801X blends, and these results are summarized in Table 2. PLA 3801X exhibited T_g at 52 °C, T_m at 142 and 152 °C, and T_{mc} at 98 °C. In the blends, the incorporation of the PLA resulted in no significant changes in T_m as similar with 4032D, but it has a remarkable influence on crystallization. Such results may be influenced by talc contained in the

PLA.^{19,20} In contrast to 4032D blends, all the 3801X blends show two endo-thermal peaks around 230 °C. It means that PCF-co-EF formed perfect crystals under the influence of PLA 3801X. To investigate crystallization kinetics of the 3801X blends in more detail, further non-isothermal crystallization kinetics were investigated.

Equilibrium Melting Temperature. When analyzing crystallization kinetics, the samples are heated beyond the equilibrium melting temperature (T_m^0) to melt completely and erase thermal history. If row nuclei, such as expanded chain, are remained in a melt-state, it can affect the crystallization kinetics.²¹ In this study, T_m^0 was obtained using the Hoffman-Weeks equation as follow (1):

$$T_m = \frac{T_c}{2\beta} + T_m^0 \left[1 - \frac{1}{2\beta} \right] \quad (1)$$

where T_m^0 is the equilibrium melting temperature and β is a constant depending on lamella thickness. Figure 4 shows the endothermic peaks of PCF-co-EF isothermal crystallization at

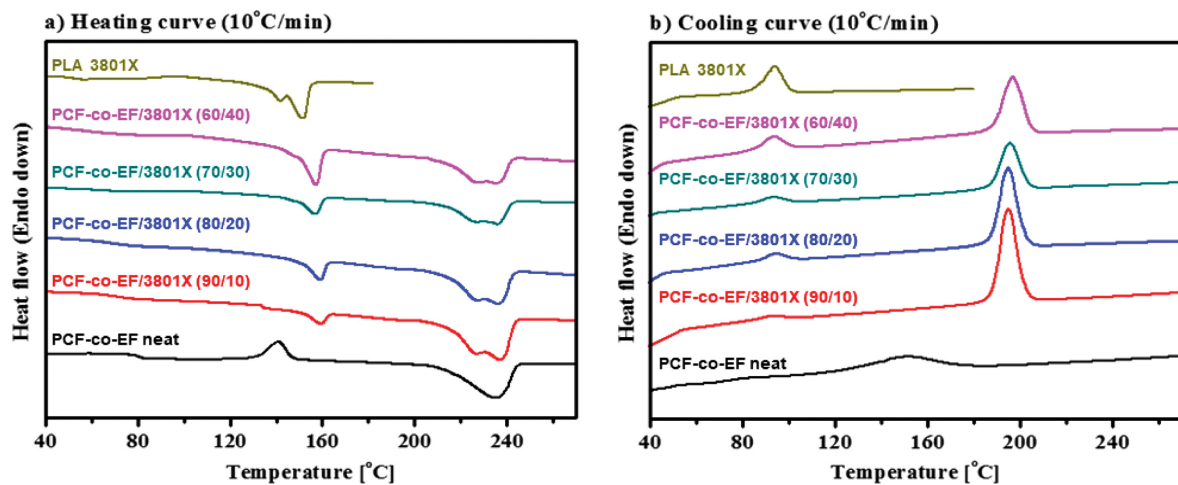


Figure 3. DSC thermograms of PCF-co-EF/PLA 3801X blends: (a) heating scan; (b) cooling scan.

Table 2. Thermal Transition Parameters of PCF-co-EF/PLA 3801X Blends

DSC (10 °C/min)	Heating				Cooling	
	T_g	T_{cc}	T_m		T_{mc}	
PLA 3801X	52	-	142, 152		98	
PCF-co-EF/3801X (90/10)	-	-	148, 157	228, 235	95	197
PCF-co-EF/3801X (80/20)	-	-	157	227, 236	95	196
PCF-co-EF/3801X (70/30)	-	-	159	227, 236	95	196
PCF-co-EF/3801X (60/40)	-	-	159	227, 237		196
PCF-co-EF	80	141	235			154

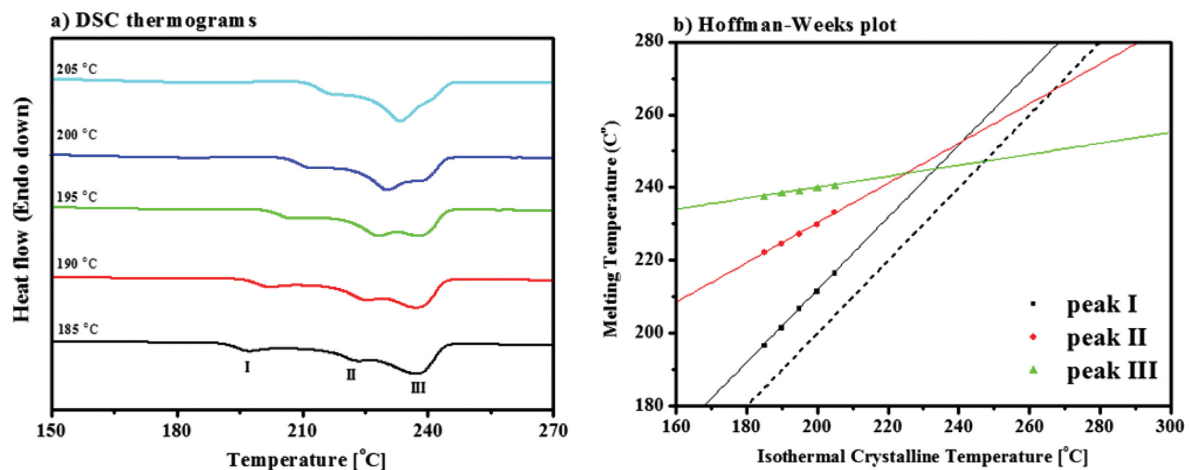


Figure 4. Determination of equilibrium melting temperature of PCF-co-EF: (a) DSC heating thermograms of PCF-co-EF isothermal crystallized at specific crystallization temperature (heating rate=10 °C/min); (b) Hoffman-Weeks plot based on peak II.

different T_c . Such peaks related to the melting of the crystals with different crystal perfection; the peak I, generally observed at about 10 °C above T_c , is caused by the melting of crystallized portions in the amorphous phase, peak II is that of primary crystal formed at designated T_c , and peak III is that of

recrystallized portion during DSC heating scan.^{22,23} In the PCF-co-EF, the peak II becomes clear with increasing T_c , which indicates that peak II is caused by melting of major crystal. According to the Hoffman-Weeks equation, T_m^0 can be calculated by the extrapolation of the T_m (peak II) versus T_c result-

ing from the $T_m=T_c$ curve as shown in Figure 4 (b). PCF-co-EF exhibited the T_m^0 at 267 °C.

Non-isothermal Crystallization Kinetics. Avrami equation is commonly used to describe the crystallization kinetics of polymer. It has below form (2) and is generally transformed into double-logarithmic function (3) to calculate the Avrami exponent:

$$X(t) = 1 - \exp(-Z_t t^n) \quad (2)$$

$$\log[-\ln(1-X(t))] = \log Z_t + n \log(t) \quad (3)$$

where t is the crystallization time, $X(t)$ is the relative crystallinity as a function of time t , Z_t is the kinetic crystallization rate, and n is the Avrami exponent.^{24,25} But, because the Avrami equation is based on isothermal crystallization kinetics, several methods have been proposed to study the non-isothermal crystallization kinetics. Among them, Ozawa equation²⁶ and Jeziorny equation¹⁵ have been widely considered. In this study, the Jeziorny equation was used to describe the non-isothermal crystallization of the blends. In a similar way with isothermal crystallization kinetics analysis, non-isothermal crystallization kinetics also can be analyzed by using the Avrami equation with a consideration of relationship between crystallization time t and temperature T (4):

$$t = \frac{T_0 - T}{R} \quad (4)$$

where T_0 is the initial temperature when crystallization begins ($t=0$) and R is the cooling rate. But, Jeziorny suggested that the value of kinetic crystallization rate (Z_t) should be corrected, considering the non-isothermal character during crystallization. He introduced the R to correct the kinetic crystallization rate (Z_c) as shown (5):

$$\log Z_c = \frac{\log Z_t}{R} \quad (5)$$

The curves of $\log[-\ln(1-X(t))]$ versus $\log(t)$ at various cooling rates are depicted in Figure 5. It shows all the curves exhibit linear form with some deviations. It is not available for all crystallization areas because of sensitivity to error at both low and high degree of crystallization.^{27,28} Thus, in this study, the range of $-2 < \log[-\ln(1-X(t))] < 0$ was considered to calculate the kinetic parameters. Half-time of crystallization ($t_{1/2}$) value was obtained when the $X(t)$ is equal to 50%. In the PCF-co-EF, Avrami exponents n varied from 2.1 to 3.1 as shown in Table 3. It indicates that PCF-co-EF crystallization occurs with two- or three-dimensional growth type.²² In the blends, the n values are higher than that of the PCF-co-EF at the same cooling rate, which indicates that the PLA 3801X (maybe the talc

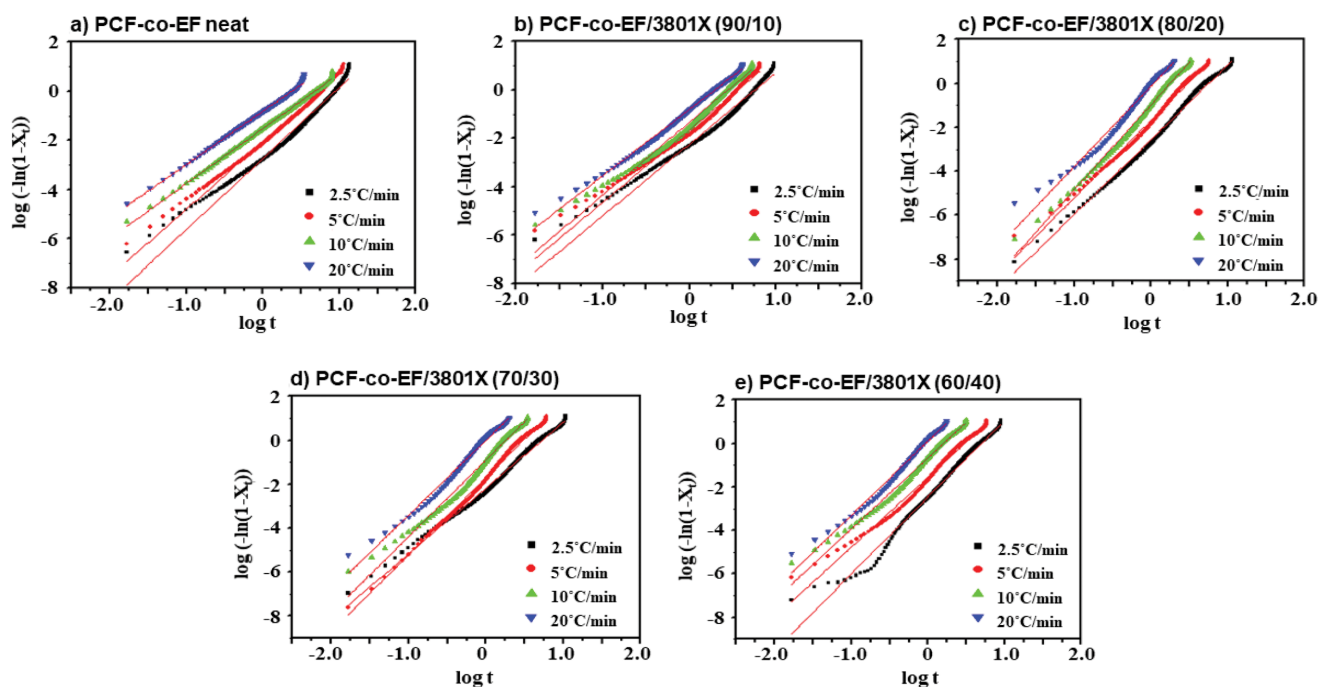


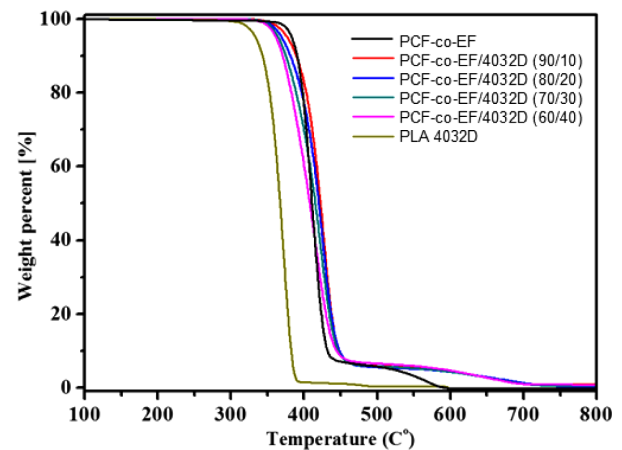
Figure 5. Plots of $\log[-\ln(1-X(t))]$ versus $\log(t)$ of PCF-co-EF/PLA3801X blends at various cooling rates.

Table 3. Non-isothermal Crystallization Kinetics Parameters of PCF-co-EF/PLA3801X Blends based on the Jeziorny Method

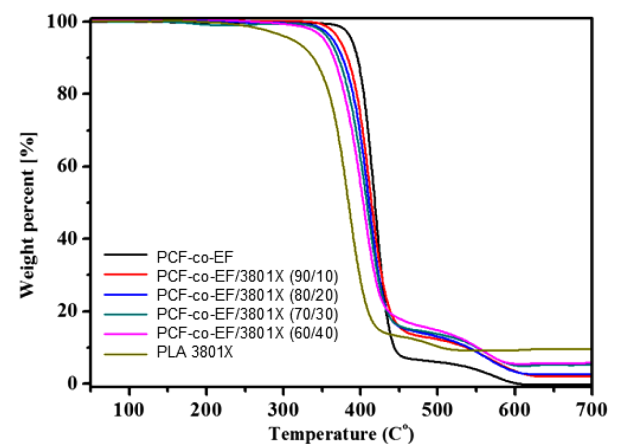
3801X blends	R (°C/min)	n	Z_c	$t_{1/2}$
PCF-co-EF	2.5	3.2	0.0580	8.0
	5	2.7	0.3715	5.3
	10	2.2	0.7064	4.0
	20	2.1	0.9092	2.1
PCF-co-EF/3801X (90/10)	2.5	3.3	0.0904	5.3
	5	3.4	0.4089	3.3
	10	3.5	0.7312	2.5
	20	3.0	0.9264	1.7
PCF-co-EF/3801X (80/20)	2.5	4.0	0.0988	4.4
	5	4.3	0.4289	2.5
	10	4.6	0.8008	1.5
	20	4.7	1.0043	0.9
PCF-co-EF/3801X (70/30)	2.5	3.6	0.1013	4.3
	5	4.2	0.4410	2.4
	10	4.6	0.8022	1.4
	20	4.3	1.0228	0.8
PCF-co-EF/3801X (60/40)	2.5	3.8	0.1081	4.1
	5	3.9	0.4656	2.4
	10	4.0	0.8609	1.3
	20	4.2	1.0314	0.8

contained in PLA) acts as a nucleating agent for the blend matrix. They ranged from 3.0 to 4.7. Such results maybe due to the spherulite impingement and crowding, or the complicated nucleation types and growth form of spherulite.²⁹ They also exhibited a higher Z_c and $t_{1/2}$ than PCF-co-EF at the same cooling rate.

Thermogravimetric Analysis. Thermal stability of the blends was analyzed by comparing a temperature where the weight loss reaches 5 wt% ($T_{d,95wt\%}$) and at maximum decomposition rate ($T_{d,max}$). In Figure 6, there is distinct difference between thermal degradation behavior of PCF-co-EF and PLA4032D. PCF-co-EF exhibited the $T_{d,95wt\%}$ at 385 °C and $T_{d,max}$ at 411 °C, while PLA exhibited the $T_{d,95wt\%}$ at 334 °C and $T_{d,max}$ at 371 °C. Interestingly, while the $T_{d,95wt\%}$ decreased with incorporation of PLA in the blends, the $T_{d,max}$ increased as shown in Table 4. Although onset of degradation was accelerated due to the PLA in the blends, it delayed thermal degradation of PCF-co-EF. As for PLA 3801X, it starts thermal

**Figure 6.** TGA thermograms of PCF-co-EF/PLA 4032D blends.**Table 4. Decomposition Temperatures at 5% Weight Loss ($T_{d,95wt\%}$) and Maximum Rate ($T_{d,max}$) of PCF-co-EF/PLA(4032D) Blends**

4032D blends	$T_{d,95wt\%}$ (°C)	$T_{d,max}$ (°C)
PCF-co-EF	385	411
PCF-co-EF/4032D (90/10)	378	430
PCF-co-EF/4032D (80/20)	370	427
PCF-co-EF/4032D (70/30)	365	425
PCF-co-EF/4032D (60/40)	362	419
PLA 4032D	334	371

**Figure 7.** TGA Thermograms of PCF-co-EF/PLA 3801X blends.

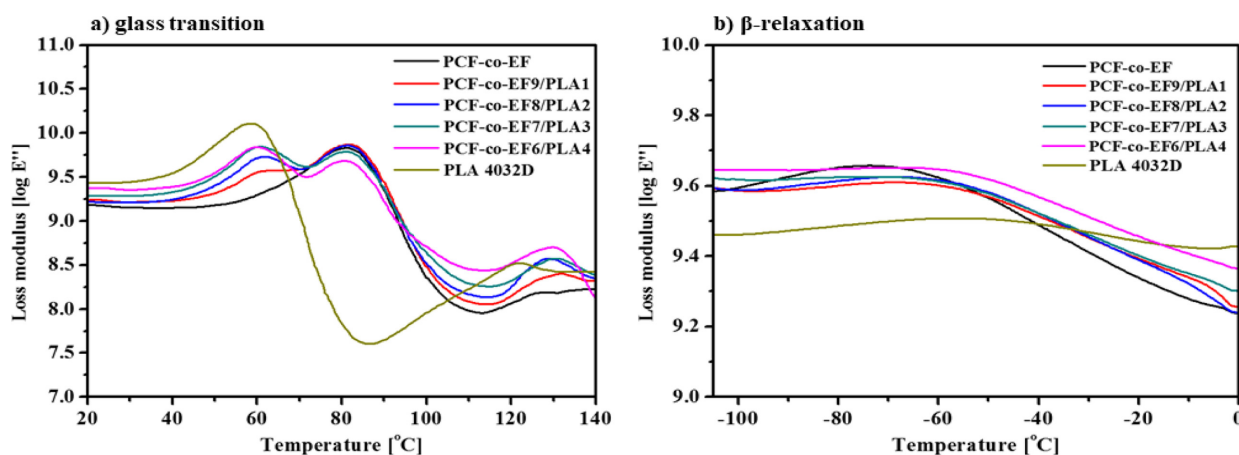
degradation at about 230 °C while its $T_{d,max}$ was higher than that of 4032D grade as shown in Figure 7. The quick degradation of PLA 3801X maybe due to plasticizers contained in it. In contrast to 4032D blends, the 3801X blends show decrease in both $T_{d,95wt\%}$ and $T_{d,max}$ with incorporation of PLA as shown in Table 5.

Table 5. Decomposition Temperatures at 5% Weight Loss ($T_{d,95wt\%}$) and Maximum Rate ($T_{d,max}$) of PCF-co-EF/PLA(3801X) Blends

3801X blends	$T_{d,95wt\%}$ (°C)	$T_{d,max}$ (°C)
PCF-co-EF	385	411
PCF-co-EF/3801X (90/10)	385	409
PCF-co-EF/3801X (80/20)	369	406
PCF-co-EF/3801X (70/30)	358	404
PCF-co-EF/3801X (60/40)	357	402
PLA 3801X	348	377

Dynamic Mechanical Analysis. To investigate the relaxation transition of the blends, dynamic mechanical thermal behavior was investigated using DMA. Polyesters generally show two, or often three, relaxation transition below T_m ; the highest relaxation transition (α -relaxation) is the glass transition, which is due to the cooperative motion of several molecular segments (micro-Brownian chain motion), and the other lower relaxation transition (β -relaxation) is the sub-glass transition, which is due to the local rotational motions of the

main chain. The $\tan \delta$ curve is commonly used to determine the relaxation transition temperature, but in fact, the value is different from that of storage modulus and loss modulus. It corresponds more closely to the transition at the midpoint of the decreasing of storage modulus curve.³⁰ Considering this problem, the loss modulus was chosen to determine relaxation transition. Figure 8 shows the loss modulus of the 4032D blends below T_m , and their characteristic peaks are summarized in Table 6. PCF-co-EF exhibited the T_g at 84 °C, and PLA 4032D exhibited it at 59 °C. In the blends, each T_g was observed between that of neat polymers. Such results indicate that partial compatibility exists in the blends although there is no remarkable change in the T_g , as discussed in the morphology result.³¹ The other relaxation peak can be observed below 0 °C. PCF-co-EF exhibited the β -relaxation at -74 °C, and it increased with incorporation of the PLA. It is assumed that the PLA hinder the carbonyl motions of PCF-co-EF, and it may result in brittleness of the blends. These behaviors were also shown in the storage modulus as shown in Figure 10(a). With incorporation of the PLA, the storage modulus at RT increased and it means there was no effect of PLA 4032D on

**Figure 8.** Loss modulus of PCF-co-EF/PLA 4032D blends at below T_m : (a) glass transition temperature; (b) β -relaxation.**Table 6. Summarized Result of Dynamic Mechanical Thermal Analysis for PCF-co-EF/PLA(4032D) Blends**

4032D Blends	$T_{d,95wt\%}$ (°C)		Storage modulus at 30 °C (log E')
	β -relaxation (°C)	T_g (°C)	
PCF-co-EF	-74	84	10.69
PCF-co-EF/4032D (90/10)	-70	61 84	10.73
PCF-co-EF/4032D (80/20)	-68	62 84	10.77
PCF-co-EF/4032D (70/30)	-66	60 82	10.80
PCF-co-EF/4032D (60/40)	-66	61 80	10.83
PLA 4032D	-56	59	10.94

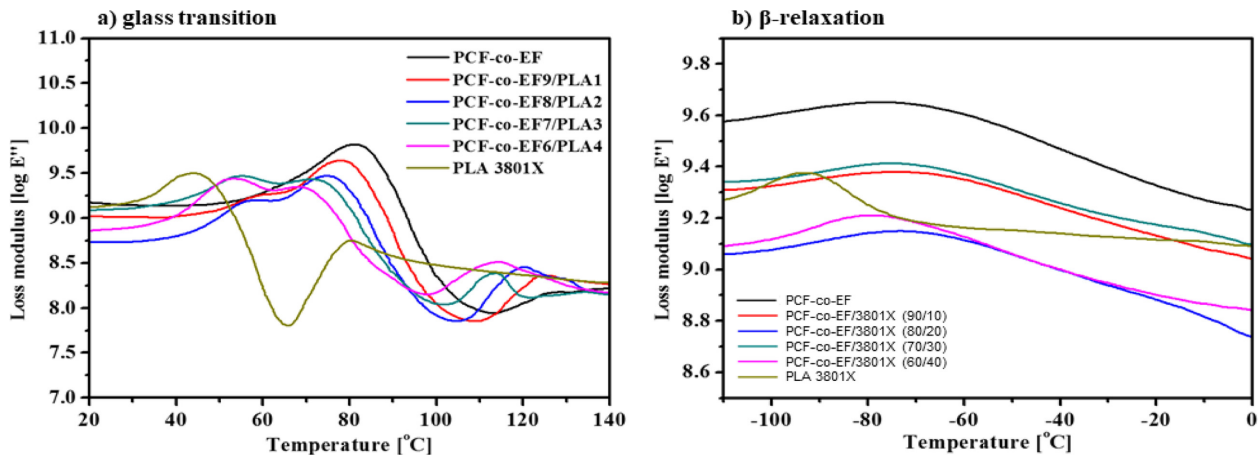


Figure 9. Loss modulus of PCF-co-EF/PLA 3801X blends at below T_m : (a) glass transition temperature; (b) β -relaxation.

Table 7. Summarized Result of Dynamic Mechanical Thermal Analysis for PCF-co-EF/PLA(3801X) Blends

3801X blends	$T_{d,95w1\%}$ (°C)		Storage modulus at 30°C (log E')
	β -relaxation(°C)	T_g (°C)	
PCF-co-EF	-74	84	10.69
PCF-co-EF/3801X (90/10)	-72	59 79	10.48
PCF-co-EF/3801X (80/20)	-73	57 76	10.42
PCF-co-EF/3801X (70/30)	-74	55 73	10.42
PCF-co-EF/3801X (60/40)	-76	53 69	10.40
PLA 3801X	-89	44	10.26

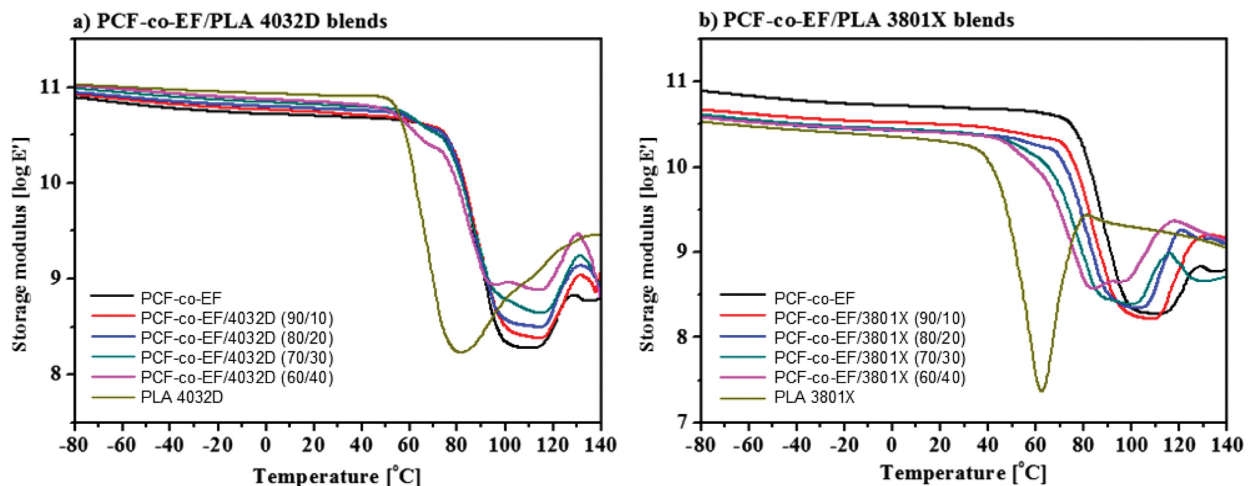


Figure 10. Storage modulus of the blends of below T_m : (a) 4032D blends; (b) 3801X blends.

improving inherent brittleness.

Figure 9 shows the loss modulus of the 3801X blends below T_m , and their characteristic peaks are summarized in Table 7. PLA 3801X exhibited the T_g at 44 °C. In the blends, there was remarkable change in the T_g . They gradually moved toward

each other, which means the 3801X blends also can be determined to be compatible as stated earlier. Also, PLA 3801X exhibited the β -relaxation at -89 °C, which is lower than that of PLA 4032D. It means that the more free chain motion of PLA 3801X results in a decrease of β -relaxation in the blends. Stor-

age modulus also decreased with incorporation of PLA 3801X as shown in Figure 10(b). Such results indicate that PLA 3801X is effective in improving brittleness.

Conclusions

PCF-co-EF, a new type of PEF copolymer, was melt blended with two types of PLA polymers; one is neat PLA (4032D) and the other is PLA with talc filler and some of additives (3801X). The FE-SEM results manifested that the PCF-co-EF is partially compatible with PLA. Especially PLA 3801X showed better compatibility than PLA 4032D. In thermal properties, both of the PLA polymers occurred T_c shift in the blends which is directly related to crystallization. In more details, non-isothermal crystallization kinetic analysis of the 3801X blends proved that the PLA 3801X accelerates the blends' crystallization rate and the PCF-co-EF/3801X (60/40) blend, which had high PLA content, showed the fastest crystallization rate. Dynamic mechanical analysis showed the two relaxation temperature. The higher relaxation temperature (T_g) confirmed compatibility of the blends and lower relaxation temperature (β -relaxation) confirmed the improvement of ductility of the 3801X blends. But, there is no effect on ductility for 4032D blends.

As a result, this study shows that PLA is an encouraging material for PCF-co-EF resins in considering the compatibility between PLA and PCF-co-EF. However, inorganic filler contained in PLA can enhance the properties such as crystallization rate and ductility. This results proves that inorganic filler like talc is an essential material for PCF-co-EF/PLA blends to overcome their drawbacks.

Even though furan-based polyesters needs more challenges to become commercialized, the results in this study demonstrated that PCF-co-EF/PLA blends can be a promising pioneer for a new trend bio-based polyester which will replace fossil-based polyesters.

References

1. L. Wu, R. Mincheva, Y. Xu, J. M. Raquez, and P. Dubois, *Biomacromolecules*, **13**, 2973 (2012).
2. T. Werpy and G. Peterson, *Top Value Added Chemicals from Biomass*, U.S. Department of Energy, Washington DC, 2004.
3. S. Burgess, J. Leisen, B. Kraftschik, C. Mubarak, R. Kriegel, and W. Koros, *Macromolecules*, **47**, 1383 (2014).
4. M. Vannini, P. Marchese, A. Celli, and C. Lorenzetti, *Green Chem.*, **17**, 4162 (2015).
5. J. Ma, Y. Pang, M. Wang, J. Xu, H. Ma, and X. Nie, *J. Mater. Chem.*, **22**, 3457 (2012).
6. J. Zhu, J. Cai, W. Xie, P. H. Chen, M. Gazzano, M. Scandola, and R. A. Gross, *Macromolecules*, **46**, 796 (2013).
7. B. Wu, Y. Xu, Z. Bu, L. Wu, B. G. Li, and P. Dubois, *Polymer*, **55**, 3648 (2014).
8. G. Z. Papageorgiou, V. Tsanaktsis, D. G. Papageorgiou, K. Chrissafis, S. Exarhopoulos, and D. N. Bikiaris, *Eur. Polym. J.*, **67**, 383 (2015).
9. J. M. Raquez, Y. Habibi, M. Murariu, and P. Dubois, *Prog. Polym. Sci.*, **38**, 1504 (2013).
10. L. Shen, J. Haufe, and M. K. Patel, Product Overview and Market Projection of Emerging Bio-based Plastics. PRO-BIP 2009, Final Report, Report Commissioned by European Polysaccharide Network of Excellence (EPNOE) and European Bioplastics, Group Science, Technology and Society, Universiteit Utrecht, The Netherlands, 2009.
11. H. Liu and J. Zhang, *J. Polym. Sci., Part B: Polym. Phys.*, **49**, 1051 (2011).
12. R. M. Taib, Z. A. Ghaleb, and Z. A. Mohd Ishak, *J. Appl. Polym. Sci.*, **123**, 2715 (2012).
13. R. M. Taib, H. M. Hassan, and Z. A. Mohd Ishak, *Polym. Plast. Technol.*, **53**, 199 (2014).
14. J. D. Hoffman and J. J. Weeks, *J. Res. Natl. Bur. Stand. Sect A*, **66**, 13 (1962).
15. A. Jeziorny, *Polymer*, **19**, 1142 (1978).
16. I. Aravind, A. Boumod, Y. Grohens, and S. Thomas, *Ind. Eng. Chem. Res.*, **49**, 3873 (2010).
17. H. Xiao, W. Lu, and J. T. Yeh, *J. Appl. Polym.*, **112**, 3754 (2009).
18. R. Elenga, R. Seguela, and F. Rietsch, *Polymer*, **32**, 1975 (1991).
19. S. Karrad, J. M. L. Cuesta, and A. Crespy, *J. Matl. Sci.*, **33**, 453 (1998).
20. J. Garcia-Martinez, O. Laguna, S. Areso, and E. P. Collar, *J. Appl. Polym. Sci.*, **81**, 625 (2001).
21. J. D. Menczel, L. Judovits, R. B. Prime, H. E. Bair, M. Reading, and S. Swier, "Differential Scanning Calorimetry (DSC)", in *Thermal Analysis of Polymers: Fundamentals and Applications*, J. D. Menczel and R. B. Prime, Editors, John Wiley & Sons Inc., Chapter 2 (2009).
22. M. Liu, Q. Zhao, Y. Wang, C. Zhang, Z. Mo, and S. Cao, *Polymer*, **44**, 2537 (2003).
23. M. C. Righetti and M. Pizzoli, *Macromol. Chem. Phys.*, **199**, 2063 (1998).
24. M. Avrami, *J. Chem. Phys.*, **8**, 212 (1939).
25. M. Avrami, *J. Chem. Phys.*, **9**, 177 (1941).
26. T. Ozawa, *Polymer*, **12**, 150 (1971).
27. J. J. Kolstad, *J. Appl. Polym. Sci.*, **62**, 1079 (1996).
28. T. Wan, L. Chen, Y. Chua, and X. Lu, *J. Appl. Polym. Sci.*, **94**, 1381 (2004).
29. H. Zou, L. Wang, C. Yi, and H. Gan, *Polym. Int.*, **60**, 1349 (2011).
30. R. P. Chartoff, J. D. Menczel, and S. H. Dillman, "Dynamic Mechanical Analysis", in *Thermal Analysis of Polymers: Fundamentals and Applications*, J. D. Menczel and R. B. Prime, Editors, John Wiley & Sons Inc., Chapter 5 (2009).
31. H. R. Kim, B. U. Nam, and Y. H. Kim, *WIT Transact. Eng. Sci.*, **88**, 648 (2014).